Organic LETTERS

Letter

pubs.acs.org/OrgLett

Mechanistic Insights on Iodine(III) Promoted Metal-Free Dual C−H Activation Involved in the Formation of a Spirocyclic Bis-oxindole

A. Sreenithya and Raghavan B. Sunoj*

Department of Chemistry, Indian Institute of Technology Bombay, Powai, Mumbai 400076, India

Supporting Information

ABSTRACT: The mechanism of a metal-free, phenyliodine(III) bis(trifluoroacetate) promoted, dual aryl C−H activation of an anilide to a spirocyclic bis-oxindole is examined using density functional theory (M06-2X). The most preferred pathway proceeds through the involvement of a novel iodonium ion intermediate and a pivotal trifluoroacetate counterion. The two sequential aryl C−H activations, assisted by trifluoroacetate as well as the superior leaving group ability of PhI, facilitate the formation of spirocyclic bis-oxindole.

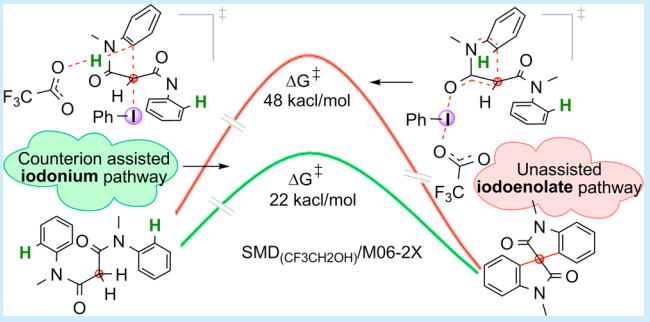

In keeping with the contemporary emphasis on environmentally benign greener reactions, the quest for transition-metal-free coupling protocols under mild reaction conditions has increased considerably. An efficient alternative to transition metal catalyzed C−C and C−heteroatom coupling reactions[1] that emerged in recent years[2] is the use of hypervalent iodine(III) reagents. Iodine reagents, such as phenyliodine(III) diacetate (PIDA) and phenyliodine(III) bis(trifluoroacetate) (PIFA), have been successfully employed in oxidative C−C and C−X (X = O, N, S) coupling reactions.[3−6] The chemistry of hypervalent iodine(III) banks on the strongly electrophilic nature of iodine, rendering it susceptible to nucleophilic attack in addition to the ability of phenyl iodide to function as a superleaving group. Although significant advances have been made in hypervalent iodine chemistry, mechanistic clarity on many of these reactions continues to remain weak.[7]

While there have been several elegant examples of hypervalent iodine mediated reactions, one of the most recent reports by Zhao et al. deserves special attention.[8] This reaction, as shown in Scheme 1, employed PIFA for the oxidative coupling in an anilide leading to a spiro bis-oxindole framework. The reaction offers a hypervalent iodine promoted metal-free $C(sp^2)-C(sp^3)$ coupling strategy. More importantly, the resulting spiro bis-oxindoles are very important synthetic targets owing to their potential as biologically active molecules.[9] Our long-standing interest toward understanding the mechanism of organocatalytic reactions[10] and the conspicuous scarcity of mechanistic studies in this emerging domain motivated us to examine the mechanism of this iodine(III) promoted spirocyclization by using density functional theory methods. In particular, we intend to shed light on the energetics, nature of key intermediates, and transition states involved in the reaction. Mechanistic insights presented here could help further developments with this class of reactions as well as contribute to the design of newer hypervalent iodine reagents, including asymmetric variants.

Scheme 1. Phenyliodine(III) Bis(trifluoroacetate) (PIFA) Mediated Intramolecular Oxidative Coupling Reaction of Anilide Derivatives to a Spiro Bis-oxindole Framework (ref 8)

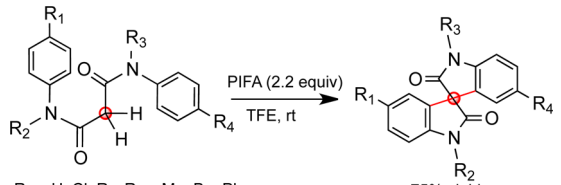

The mechanism of PIFA promoted intramolecular dual C−H activation in a dianilide yielding a spirocyclic product is explored using the DFT(M06-2X) level of theory. All geometries were optimized in the condensed phase using the continuum dielectric constant of trifluoroethanol (TFE).[11] The Gibbs free energies obtained at the $SMD_{(TFE)}$/M06-2X/LANL2DZ(I),6-31G**(for all other atoms) level is employed for discussions. In the absence of mechanistic generalizations for iodine(III) promoted reactions, we envisaged different likely pathways, as shown in Scheme 2. The reaction can begin with a nucleophilic attack of the carbonyl oxygen of the anilide on the hypervalent iodine center leading to the displacement of one of the trifluoroacetate ions (CF_3COO^-). The resulting adduct $\mathbf{2}_a$ is an iodinated substrate interacting with CF_3COO^-. The ensuing proton abstraction by CF_3COO^- from the activated methylene provides an iodo enolate intermediate $\mathbf{3}_a$. Now, $\mathbf{3}_a$ can either (i) undergo a direct ring closure with a concomitant expulsion of PhI and CF_3COO^- to give intermediate **7** (Pathway I) or (ii) convert to an iodonium intermediate $\mathbf{4}_a$ upon changing from the

Received: October 29, 2014
Published: November 24, 2014

dx.doi.org/10.1021/ol503161g | Org. Lett. 2014, 16, 6224−6227

Scheme 2. Mechanistic Possibilities for the Oxidative Cross-Coupling Reaction of an Anilide Derivative to Spiro Bis-oxindole

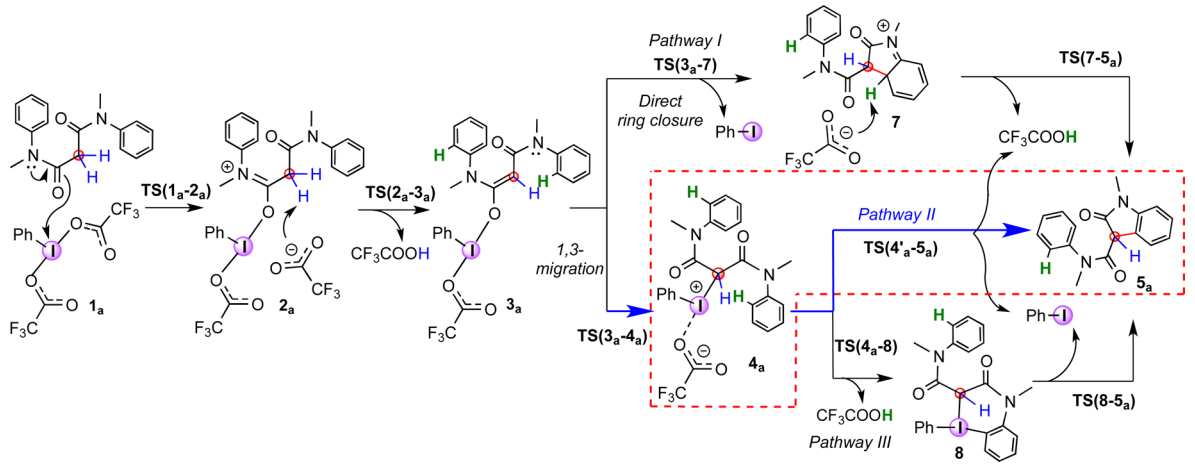

O-iodoenolate to a *C*-iodonium enolate (1,3-migration). $\mathbf{4_a}$ can subsequently undergo a C−C bond formation between the methylenic carbon and *ortho*-aryl carbon of the *N*-phenyl group, which would be accompanied by the abstraction of the *ortho* aryl C−H by the counterion CF_3COO^- to yield mono-oxindole $\mathbf{5_a}$ (Pathway II). Alternatively, the weakly interacting CF_3COO^- counterion in $\mathbf{4_a}$ can be thought of as promoting an acetate-assisted *ortho* C−H activation through a cycloiodination deprotonation process leading to an iodacyclic intermediate (**8**) (Pathway III).

A more detailed mechanistic description is presented below. In the very first step, the substrate combines with the iodine(III) reagent to form a substrate−PIFA adduct $\mathbf{2_a}$. This occurs by the substitution of one of the CF_3COO^- on iodine by the incoming anilide via **TS**($\mathbf{1_a}$-$\mathbf{2_a}$). The deprotonation of the methylenic C−H by the departing CF_3COO^- through **TS**($\mathbf{2_a}$-$\mathbf{3_a}$) then provides an *O*-iodoenolate ($\mathbf{3_a}$).[12] In line with one of the most commonly invoked mechanisms, we have first examined an intramolecular cyclization of $\mathbf{3_a}$ to a dearomatized intermediate **7**. This cyclization is accompanied by the expulsion of PhI and the second CF_3COO^-. Intermediate **7** upon deprotonation by the CF_3COO^- present in the immediate neighborhood can rearomatize to give a mono-oxindole $\mathbf{5_a}$. For the sake of clarity of discussions, the above-mentioned mechanism is termed as pathway I.

The Gibbs free energies of the key transition states and intermediates in different plausible pathways considered in this study are provided in Figure 1. It is readily evident that the barrier to cyclization of *O*-iodoenolate $\mathbf{3_a}$ to dearomatized **7** is prohibitively high (~48 kcal/mol), particularly for a reaction under milder conditions. Such high barriers are due to the energy penalty associated with the formation of a dearomatized intermediate such as **7**. The distortion of the aryl ring that participates in ring closure is noticeable from the optimized geometry **TS**($\mathbf{3_a}$-**7**) given in Figure 2.[13] In view of such higher energies noted for the conventional cyclization route, we have examined alternative pathways.

Instead of a direct ring closure, the *O*-iodoenolate $\mathbf{3_a}$ can undergo a 1,3-migration of the hypervalent iodine to give a *C*-iodoniumenolate $\mathbf{4_a}$. It is noticed from Figure 1 that the corresponding transition state **TS**($\mathbf{3_a}$-$\mathbf{4_a}$) is much lower in energy as compared to **TS**($\mathbf{3_a}$-**7**). In **TS**($\mathbf{3_a}$-$\mathbf{4_a}$) breaking O−I and forming C−I bond distances are respectively 2.49 and 2.68 Å. On 1,3-migration, enolate negative charge tends to localize more on

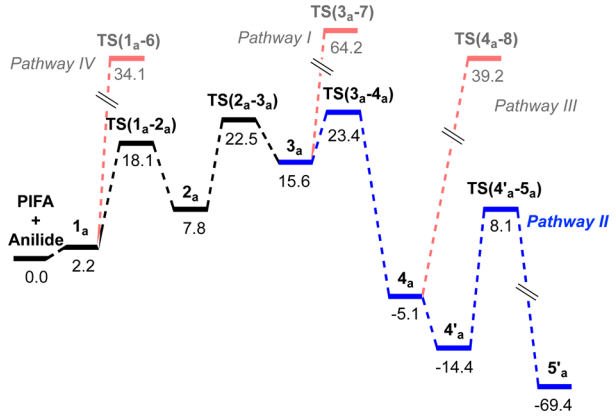

Figure 1. Free energy (kcal/mol) profiles of pathways I through IV toward the formation of the mono-oxindole product from anilide obtained at the $SMD_{(TFE)}$/M06-2X/LANL2DZ, 6-31G** level of theory.

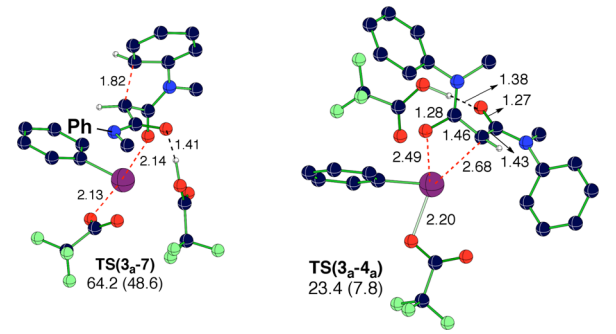

Figure 2. $SMD_{(TFE)}$/M06-2X/LANL2DZ,6-31G** optimized geometries of **TS**($\mathbf{3_a}$-**7**) and **TS**($\mathbf{3_a}$-$\mathbf{4_a}$). Relative Gibbs free energy (kcal/mol) with respect to dianilide and PIFA are provided. Activation barrier with respect to the preceding intermediate is given in parentheses.

the methylene carbon (natural charges on the methylene carbon of $\mathbf{3_a}$ and $\mathbf{4_a}$ are −0.599 and −0.659 respectively). A weaker hydrogen bonding between departing CF_3COOH and the *β*-carbonyl oxygen further indicates the lack of charge delocalization in $\mathbf{4_a}$ (1.62 Å) as compared to that in $\mathbf{3_a}$ (1.28 Å) and **TS**($\mathbf{3_a}$-$\mathbf{4_a}$) (1.38 Å). This pathway signifies, for the first time, the potential participation of an iodonium species in the mechanism of an iodine(III) promoted reaction. Interestingly, isolation of a stabilized bis-iodonium intermediate was recently reported by

dx.doi.org/10.1021/ol503161g | *Org. Lett.* 2014, 16, 6224−6227

Kita et al.[14] In addition to the lower kinetic barrier, the change of coordination is found to be highly feasible thermodynamically for the conversion of $\mathbf{3_a}$ to $\mathbf{4_a}$ as indicated by the computed exoergicity of 20 kcal/mol. The binding of the CF_3COO^- with iodine is found to be weaker in the resulting iodonium intermediate $\mathbf{4_a}$, which is a characteristic feature of iodonium salts (I−O distance is 2.63 Å in $\mathbf{4_a}$ whereas in $\mathbf{3_a}$ it is 2.17 Å). This species, as shown in Figure 3, can also be viewed as a combination

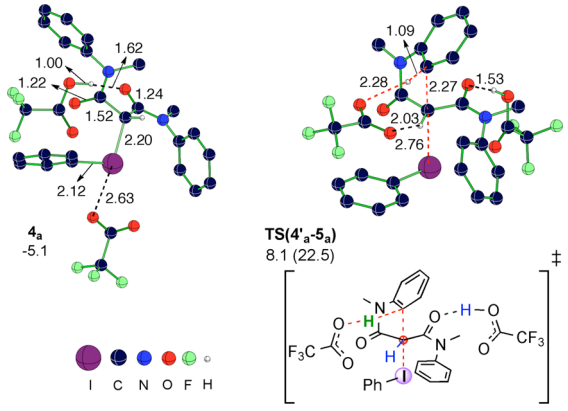

Figure 3. $SMD_{(TFE)}$/M06-2X/LANL2DZ,6-31G** optimized geometries of *C*-iodonium enolate $\mathbf{4_a}$ and $\mathbf{TS(4'_a\text{-}5_a)}$. Relative Gibbs free energy (kcal/mol) with respect to dianilide and PIFA are provided. Activation barrier with respect to the preceding intermediate is given in parenthesis.

of a cationic hypervalent iodine center and a CF_3COO^- counterion.[15] A lower energy analogue of $\mathbf{4_a}$ (~9 kcal/mol), wherein the counterion is positioned opposite to the phenyl ligand on the iodine center ($\mathbf{4'_a}$), is as well identified. The optimized geometries of these ion pair intermediates reveal that, in $\mathbf{4'_a}$, CF_3COO^- develops an improved H-bonding interaction with the acidic methylene hydrogen in addition to its weak interaction with the iodine center.[16]

The next vital step in this mechanism, denoted as pathway II, is the C−C bond formation in the iodonium intermediate $\mathbf{4'_a}$ via $\mathbf{TS(4'_a\text{-}5_a)}$. The geometric features of this transition state indicate that the bond formation between the *ortho*-carbon of the *N*-phenyl group and the methylenic carbon is accompanied by a simultaneous C−I(Ph) bond cleavage and expulsion of PhI (Figure 3). In this transition state, the *ortho* C−H of the *N*-phenyl moiety is abstracted by the CF_3COO^- counterion, yielding a product complex of mono-oxindole, PhI, and CF_3COOH (denoted as $\mathbf{5'_a}$).[17] The product designated as $\mathbf{5_a}$ in the text is the product mono-oxindole devoid of PhI, and CF_3COOH. The free energy of activation of $\mathbf{TS(4'_a\text{-}5_a)}$ is only ~22 kcal/mol (Figure 1). The change in oxidation state of iodine from III to I and the release of three neutral products provide a noticeable thermodynamic drive for the reaction through this iodonium pathway. The most important feature of $\mathbf{TS(4'_a\text{-}5_a)}$ for the C−H activation is that it avoids the involvement of a dearomatized *N*-phenyl ring as noted in pathway I discussed earlier. Instead, the CF_3COO^- assisted deprotonation and the C−C bond formation are found to follow a concerted lower energy path.[18]

After having found an important noninnocent role of the counterion in the iodonium path, we have examined another logical extension wherein CF_3COO^- assists in the *ortho* C−H activation of the *N*-phenyl group of iodonium intermediate $\mathbf{4_a}$ (pathway III).[19] The deprotonation of the aromatic C−H by CF_3COO^- leads to a six-membered iodacycle intermediate **8** (Scheme 2). Subsequent reductive elimination in **8** yields a mono-oxindole as the product by releasing a molecule of PhI. However, the Gibbs free energy barrier for the corresponding transition state $\mathbf{TS(4_a\text{-}8)}$ is as high as 44 kcal/mol (Figure 1), suggesting a highly unlikely scenario for this pathway to operate under rt reaction conditions. The optimized geometry of $\mathbf{TS(4_a\text{-}8)}$ is shown in Figure S5. Along similar lines, an alternative route wherein *ortho* C−H activation of *N*-phenyl group occurs prior to the enolate formation (pathway IV) is also probed.[20] However, the corresponding transition state is of higher energy ($\mathbf{TS(1_a\text{-}6)}$) as shown in Figure 1. On the basis of the higher barriers in all pathways (I, III, and IV), except that in the iodonium pathway, we have considered only the iodonium mechanism for the cyclization of mono-oxindole to spiro bis-oxindole.

The mono-oxindole product formed through the iodonium mechanism (pathway II) can now undergo a similar sequence of reactions to provide the final spirocyclic bis-oxindole product.[21] The most important steps, together with the corresponding energetics, leading to the spirocyclic product is shown in Scheme 3. The first key difference in the energetics is that the barrier to

Scheme 3. Iodonium Mechanism for the Oxidative Cross-Coupling in Mono-oxindole to Spiro Bis-oxindole[a]

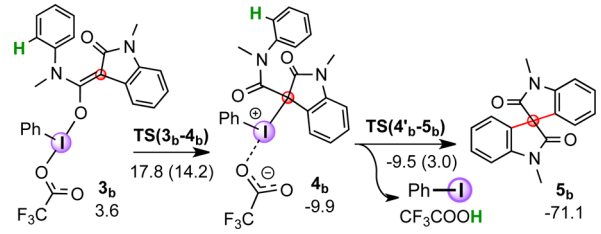

[a]Relative Gibbs free energies (kcal/mol) are with respect to $\mathbf{5_a}$ and PIFA, and the activation barrier is with respect to the preceding intermediate.

the formation of the substrate−iodine complex by the mono-oxidole via ($\mathbf{TS(1_b\text{-}2_b)}$) is 3.1 kcal/mol higher as compared to that noted earlier with the unmodified anilide involving $\mathbf{TS(1_a\text{-}2_a)}$. Similarly, the conversion of *O*-iodoenolate $\mathbf{3_b}$ to *C*-iodonium enolate $\mathbf{4_b}$ is also found to be a 7.2 kcal/mol higher barrier. However, the enolate formation ($\mathbf{(TS(2_b\text{-}3_b))}$) is 4.2 kcal/mol lower than the corresponding step in the first phase of the reaction leading up to the mono-oxindole intermediate. The other important difference is in the energetics of the ring closing C−C bond formation, leading to the spirocyclic bis-oxidole via $\mathbf{TS(4'_b\text{-}5_b)}$.[22] This step exhibits a significantly lower barrier of only 3.0 kcal/mol, which results in the formation of PhI and CF_3COOH and the final spiro bis-oxindole product.

In conclusion, the mechanism of oxidative coupling of an anilide derivative to a spiro bis-oxindole has been identified to proceed through an iodonium intermediate and a vital trifluoroacetate counterion. The participation of trifluoroacetate in the aryl C−H activation offered the energetically most preferred transition state for the C−C coupling between the methylenic and the *ortho*-aryl carbon atoms of the anilide. The insights reported here would be valuable for further developments in iodine(III) promoted C−H activation reactions.

dx.doi.org/10.1021/ol503161g | *Org. Lett.* 2014, 16, 6224−6227

■ ASSOCIATED CONTENT

Supporting Information

Cartesian coordinates of all the transition states. This material is available free of charge via the Internet at http://pubs.acs.org.

■ AUTHOR INFORMATION

Corresponding Author

*E-mail: sunoj@chem.iitb.ac.in.

Notes

The authors declare no competing financial interest.

■ ACKNOWLEDGMENTS

Generous computing time from the IIT Bombay supercomputing is acknowledged.

■ DEDICATION

Dedicated to the memory of Prof. Paul v. R. Schleyer (1930−2014).

■ REFERENCES

(1) (a) Seechurn, C. C. C. J.; Kitching, M. O.; Colacot, T. J.; Snieckus, V. *Angew. Chem., Int. Ed.* **2012**, *51*, 5062. (b) Dyker, G. *Angew. Chem., Int. Ed.* **1999**, *38*, 1698. (c) Jana, R.; Pathak, T. P.; Sigman, M. S. *Chem. Rev.* **2011**, *111*, 1417. (d) Yeung, C. S.; Dong, V. M. *Chem. Rev.* **2011**, *111*, 1215.

(2) (a) Sun, C.-L.; Shi, Z.-J. *Chem. Rev.* **2014**, *114*, 9219. (b) Mehta, V. P.; Punji, B. *RSC Adv.* **2013**, *3*, 11957.

(3) (a) Ito, M.; Kubo, H.; Itani, I.; Morimoto, K.; Dohi, T.; Kita, Y. *J. Am. Chem. Soc.* **2013**, *135*, 14078. (b) Moteki, S. A.; Usui, A.; Selvakumar, S.; Zhang, T.; Maruoka, K. *Angew. Chem., Int. Ed.* **2014**, *53*, 11060. (c) Dohi, T.; Kato, D.; Hyodo, R.; Yamashita, D.; Shiro, M.; Kita, Y. *Angew. Chem., Int. Ed.* **2011**, *50*, 3784. (d) Matcha, K.; Antonchick, A. P. *Angew. Chem., Int. Ed.* **2013**, *52*, 2082.

(4) (a) Fujita, M.; Yoshida, Y.; Miyata, K.; Wakisaka, A.; Sugimura, T. *Angew. Chem., Int. Ed.* **2010**, *49*, 7068. (b) Dohi, T.; Takenaga, N.; Nakae, T.; Toyoda, Y.; Yamasaki, M.; Shiro, M.; Fujioka, H.; Maruyama, A.; Kita, Y. *J. Am. Chem. Soc.* **2013**, *135*, 4558. (c) Zhao, F.; Liu, X.; Qi, R.; Zhang-Negrerie, D.; Huang, J.; Du, Y.; Zhao, K. *J. Org. Chem.* **2011**, *76*, 10338.

(5) (a) Manna, S.; Matcha, K.; Antonchick, A. P. *Angew. Chem., Int. Ed.* **2014**, *53*, 8163. (b) Souto, J. A.; Becker, P.; Iglesias, A.; Muñiz, K. *J. Am. Chem. Soc.* **2012**, *134*, 15505. (c) Kim, H. J.; Kim, J.; Cho, S. H.; Chang, S. *J. Am. Chem. Soc.* **2011**, *133*, 16382.

(6) C−S bond formation reactions: (a) Frei, R.; Waser, J. *J. Am. Chem. Soc.* **2013**, *135*, 9620. (b) Downer-Riley, N. K.; Jackson, Y. A. *Tetrahedron* **2008**, *64*, 7741. Reviews: (c) Zhdankin, V. V.; Stang, P. J. *Chem. Rev.* **2008**, *108*, 5299. (d) Charpentier, J.; Früh, N.; Togni, A. *Chem. Rev.* **2014**, DOI: 10.1021/cr500223h. (e) Singh, F. V.; Wirth, T. *Chem.—Asian J.* **2014**, *9*, 950. (f) Parra, A.; Reboredo, S. *Chem.—Eur. J.* **2013**, *19*, 17244.

(7) (a) Carroll, M. A.; Martín-Santamaría, S.; Pike, V. W.; Rzepa, H. S.; Widdowson, D. A. *J. Chem. Soc., Perkin Trans. 2* **1999**, 2707. (b) Su, J. T.; Goddard, W. A., III. *J. Am. Chem. Soc.* **2005**, *127*, 14146. (c) Uyanik, M.; Akakura, M.; Ishihara, K. *J. Am. Chem. Soc.* **2009**, *131*, 251. (d) Kang, Y.-B.; Gade, L. H. *J. Am. Chem. Soc.* **2011**, *133*, 3658. (e) Singh, F. V.; Rehbein, J.; Wirth, T. *ChemistryOpen* **2012**, *1*, 245. (f) Sala, O.; Lüthi, H. P.; Togni, A. *J. Comput. Chem.* **2014**, *35*, 2122. (g) Konnick, M. M.; Hashiguchi, B. G.; Devarajan, D.; Boaz, N. C.; Gunnoe, T. B.; Groves, J. T.; Gunsalus, N.; Ess, D. H.; Periana, R. A. *Angew. Chem., Int. Ed.* **2014**, *53*, 10490.

(8) Wang, J.; Yuan, Y.; Xiong, R.; Zhang-Negrerie, D.; Du, Y.; Zhao, K. *Org. Lett.* **2012**, *14*, 2210.

(9) (a) Tan, B.; Candeias, N. R.; Barbas, C. F., III. *Nat. Chem.* **2011**, *3*, 473. (b) Tessier, J. D.; O'Bryan, E. A.; Schroeder, T. B. H.; Cohen, D. T.; Scheidt, K. A. *Angew. Chem., Int. Ed.* **2012**, *51*, 4963. (c) Santos, M. M. M. *Tetrahedron* **2014**, DOI: 10.1016/j.tet.2014.08.005.

(10) (a) Sharma, A. K.; Sunoj, R. B. *Angew. Chem., Int. Ed.* **2010**, *49*, 6373. (b) Jindal, G.; Sunoj, R. B. *Angew. Chem., Int. Ed.* **2014**, *53*, 4432. (c) Reddi, Y.; Sunoj, R. B. *Org. Lett.* **2012**, *14*, 2810. (d) Sunoj, R. B. *WIREs Comp. Mol. Sci.* **2011**, *1*, 920.

(11) (a) Frisch, M. J.; et al. Gaussian09, revision A.02; Gaussian, Inc.: Wallingford, CT, 2004. (b) More details of computational methods are given in the Supporting Information (SI). (c) Additional single-point energy calculations ($SMD_{(TFE)}$/M06-2X/DGDZVP,6-311+G**) as well as full geometry optimizations ($SMD_{(TFE)}$/M06-2X/DGDZVP,6-31G**) for important stationary points using an all-electron basis set for iodine revealed similar trends in energy. See Tables S1 and S2 in the SI.

(12) The charge delocalization in enolate $\mathbf{3}_a$ results in an elongation of the C−O bond (1.28 Å) of the *β*-carbonyl group and a notable negative charge on the oxygen. The CF_3COOH formed as a result of proton abstraction thus develops strong hydrogen bonding with the *β*-carbonyl oxygen. See Figure S1 in the SI.

(13) Nucleus Independent Chemical Shift (NICS) calculation indicated a significant loss of aromaticity of the *N*-phenyl ring involved in the ring closure.

(14) (a) Dohi, T.; Kato, D.; Hyodo, R.; Yamashita, D.; Shiro, M.; Kita, Y. *Angew. Chem., Int. Ed.* **2011**, *50*, 3784. Likely involvement of intermediates with a C−I bond were proposed in a number of hypervalent iodine mediated reactions. (b) Kita, Y.; Okunaka, R.; Kondo, M.; Tohma, H.; lnagaki, M.; Hatanaka, K. *J. Chem. Soc., Chem. Commun.* **1992**, 429. (c) Suzuki, S.; Kamo, T.; Fukushi, K.; Hiramatsu, T.; Tokunaga, E.; Dohi, T.; Kita, Y.; Shibata, N. *Chem. Sci.* **2014**, *5*, 2754. (d) Zefirov, N. S.; Kozmin, A. S.; Kasumov, T.; Potekhin, K. A.; Sorokin, V. D.; Brel, V. K.; Abramkin, E. V.; Struchkov, Y. T.; Zhdankin, V. V.; Stang, P. J. *J. Org. Chem.* **1992**, *57*, 2433. (e) Ochiai, M.; Takeuchi, Y.; Katayama, T.; Sueda, T.; Miyamoto, K. *J. Am. Chem. Soc.* **2005**, *127*, 12244. (f) Moon, N. G.; Harned, A. M. *Tetrahedron Lett.* **2013**, *54*, 2960. (g) Pouysegu, L.; Chassaing, S.; Dejugnac, D.; Lamidey, A.-M.; Miqueu, K.; Sotiropoulos, J.-M.; Quideau, S. *Angew. Chem., Int. Ed.* **2008**, *47*, 3552. (h) Farid, U.; Malmedy, F.; Claveau, R.; Albers, L.; Wirth, T. *Angew. Chem., Int. Ed.* **2013**, *52*, 7018.

(15) The strong *trans* influence exerted by the enolate carbon coordinated to the iodine could weaken its interaction with the trifluoroacetate. (a) Sajith, P. K.; Suresh, C. H. *Inorg. Chem.* **2013**, *52*, 6046. (b) Ochiai, M.; Sueda, K.; Miyamoto, T.; Kiprof, P.; Zhdankin, V. V. *Angew. Chem., Int. Ed.* **2006**, *45*, 8203.

(16) The geometry of $\mathbf{4'}_a$ is provided in Figure S2 in the SI.

(17) The geometry of this product complex ($\mathbf{5}_a'$) is provided in Figure S3 in the SI.

(18) The Extended Intrinsic Reaction Coordinate (IRC) profile indicated the absence of any intermediates other than the product $\mathbf{5}_a$. See Figure S4 in the SI.

(19) See Scheme S1 in the SI.

(20) See Scheme S2 in the SI.

(21) See Scheme S3 in the SI.

(22) Additional details on the C−C bond formation transition states for the second ring closing step is provided in Figures S7 and S8 in the SI.